Pergamon

Cement and Concrete Research 30 (2000) 1013–1016

CEMENT AND CONCRETE RESEARCH

Effect of phosphate on the hydration of alkali-activated red mud–slag cementitious material

Chunming Gong[a,*], Nanru Yang[b]

[a]*Central Research Institute of Building and Construction, Ministry of Metallurgical Industry, Room 4, Entrance 29, 25 Yuetanbeijie, Xicheng District, Beijing 100088, People's Republic of China*

[b]*Department of Materials Science, Nanjing University of Chemical Technology, 5 Xinmufan Road, Nanjing 210009, People's Republic of China*

Received 27 October 1998; accepted 16 March 2000

Abstract

The influence of sodium phosphate on the hydration of alkali-activated red mud–slag cementitious material (AARS) is studied through microcalorimeter, X-ray diffraction (XRD), and energy dispersive spectroscopy (EDS). It is shown that sodium phosphate decreases the hydration heat evolution and retards the hydration reaction of AARS effectively. A new phase is found to form in this system. The retarding mechanism is greatly attributed to the forming of this new phase. The composition of the new phase is identified and analyzed. © 2000 Elsevier Science Ltd. All rights reserved.

Keywords: AARS; Hydration; Retardation; Phosphate

1. Introduction

In the recent years, different kinds of alkali-activated cementitious materials (AAM) have been developed because of their many advantages compared with ordinary Portland cement. There are also many reports about the researches on the hydration, hardening and properties of AAM [1,2]. In order to put them into practice, effective retarders must be blended in to make them avoid setting too fast. Now, borate and phosphate are used as retarders for AAM, and the setting time similar to OPC have been obtained. Very few papers and reports on the mechanism of these retarders are published [3,4]. In a previous paper [5], the properties of alkali-activated red mud–slag cementitious material (AARS) are reported. The function of phosphate in the hydration and hardening of AARS is studied through microcalorimeter, X-ray diffraction (XRD) and energy dispersive spectroscopy (EDS).

2. Experimental

2.1. Raw materials

Red mud is obtained from Shandong Aluminium Factory. The chemical composition is shown in Table 1. The main minerals in red mud are β-C_2S and $CaCO_3$; a small amount of $CaO{\cdot}TiO_2$ and $Na_2O{\cdot}Al_2O_3{\cdot}2SiO_2{\cdot}H_2O$ are also present. Slag was obtained from Nanjing Steel and Iron Factory, which chemical composition is shown in Table 2. Water glass (mole ratio of SiO_2 to Na_2O is 2.8) was prepared by Nanjing University of Chemical Technology. Water glass of other modulus was obtained by adding NaOH to the water glass with modulus of 2.8. Sodium phosphate was produced by Nanjing Inorganic Chemical Factory.

2.2. Preparation of sample

Pastes were made with ground red mud and slag mixed with liquid water glass in the following experiments. The ratio of water to solid (slag + red mud) was 0.24. After curing in a mold for 1 day at 20 ± 3°C, the paste was demolded and cured in water of 20 ± 3°C.

* Corresponding author. Tel.: +86-10-1380-0129-752; fax: +86-10-6226-2560.

E-mail address: yjfwdc@public.yj.cn.net (C. Gong).

PII: S0008-8846(00)00260-X

Table 1
Chemical composition of red mud (mass, %)

Composition	CaO	SiO_2	Al_2O_3	Fe_2O_3	MgO	Na_2O	K_2O	Loss I.
Percentage (%)	38.84	21.90	7.96	6.57	1.60	2.32	0.41	17.42

3. Results and discussion

3.1. Setting time

In order to cause AARS to set similarly to OPC, sodium phosphate was added. Setting time is tested with Vicat needle method according to GB1346. The influence of sodium phosphate on the setting time of AARS is shown in Fig. 1. Both initial and final setting time were prolonged with the percentage of sodium phosphate, more sharply when P_2O_5 equivalent content of sodium phosphate surpasses 0.5%. When the P_2O_5 reaches 2.0% of AARS, the material sets after 4 h, but the initial and final setting times are very close. This ensures that the setting time of this material is long enough to use in construction.

3.2. Heat evolution

The hydration heat evolution of AARS with or without sodium phosphate is tested with microcalorimeter CM 204. The weight of each sample is 10 g and the ratio of water to solid is 0.6. Experimental results are shown in Fig. 2. As in OPC, there are three main hydration heat evolution peaks (a, b and c) for each curve of AARS, in which a and b is higher and c is lower and difficult to identify. The difference from OPC is that the distance between each two peaks of AARS is shorter. It is shown in Fig. 2 that the height and width of peaks, especially the second one, greatly decrease with the increase of the percentage of sodium phosphate in AARS.

It is suggested that the hydration process of AARS is divided into four different hydration periods by the three peaks. The first peak is formed because of the moistening of AARS particles and the formation of first C-S-H through the reaction of Ca^{2+} from slag and SiO_4^{4-} from water glass. The second peak is attributed to secondary formation of C-S-H through the reaction of Ca^{2+}, Na^{+} and Mg^{2+} from solution and SiO_4^{4-} from slag. At last, the hydration reaction of AARS is controlled by the diffusion of different ions.

Table 2
Chemical composition of slag (mass, %)

Composition	CaO	SiO_2	Al_2O_3	Fe_2O_3	MgO	SO_3	Loss I.
Percentage (%)	37.99	32.53	12.86	3.97	10.57	2.10	1.37

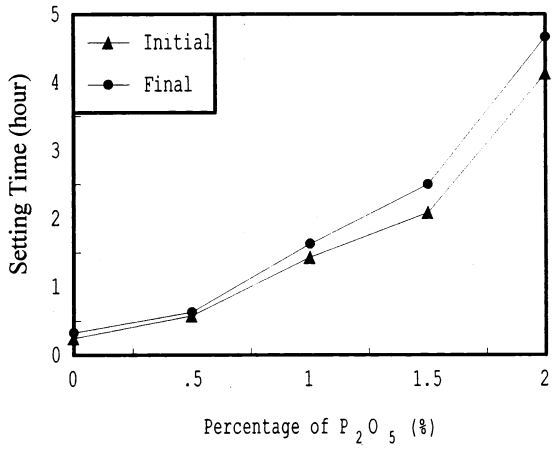

Fig. 1. Influence of P_2O_5 on the setting of AARS.

The following equations [Eq. (1,2)] can be obtained:

$$f_t = \mathrm{d}Q/\mathrm{d}t \tag{1}$$

$$Q_t = \int_0^t f_t \mathrm{d}t \tag{2}$$

where f_t is the heat evolution rate in hydration time (t) hours and Q_t is the heat evolution value in t hours.

The heat evolution value of each peak can be calculated according to Eq. (2). The results are shown in Table 3.

The time when the two peaks of each curve appear is delayed more with the increase of sodium phosphate in AARS. At the mean time, the width of each peak gets narrower. The total heat evolution value of the first two peaks decreases from 233.2 to 33.5 J/g as the percentage of P_2O_5 increases from 0% to 2%. Sodium phosphate retards the hydration reaction effectively.

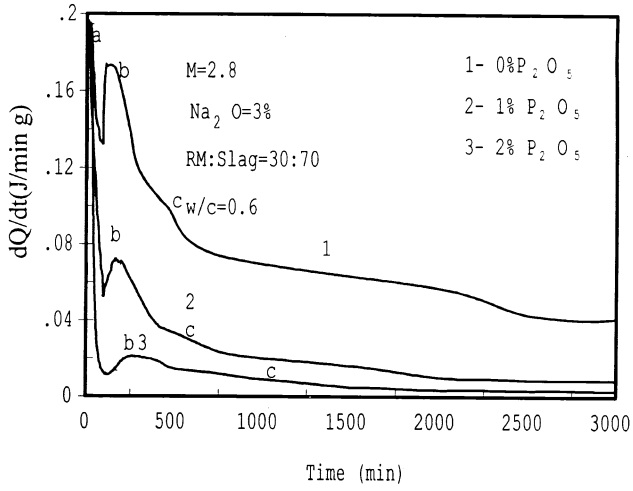

Fig. 2. Heat evolution curve of AARS.

Table 3
Heat evolution value of AARS for each peak (J/g)

	Formula			First peak			Total of other peaks		
No.	Red mud (%)	Slag (%)	P_2O_5 (%)	Situation (min)	Width (min)	Heat evolution (J/g)	Second peak (min)	Heat evolution (J/g)	Total (J/g)
H1	30	70	0	14	176	28.2	306	205.0	233.2
H2	30	70	1	16	126	14.3	310	112.2	126.5
H3	30	70	2	20	63	7.2	312	26.3	33.5

3.3. Retarding mechanism of phosphate to AARS

The AARS paste samples cured for different ages are tested with XRD at first (D/max-2b at first with the testing condition: CuK_α; 5–80° 2θ; 10°/min). Experimental results of AARS with and without sodium phosphate are shown in Fig. 3(a) and (b), respectively. It can be found by comparing Fig. 3(b) with (a) that there are some new characteristic peaks with *d* values of 0.335, 0.328 and 0.290 nm, when sodium phosphate is added. The intensity of these peaks becomes greater with curing age (from 0 min to 8 h). This phase cannot be identified with JSCP card, so it is inferred that the phase may be a new one. Sodium phosphate expedites the growth of the new phase, and this may be attributed to the retarding mechanism of sodium phosphate. It is also deduced by analyzing Fig. 3 with JSCP card that $Ca_3(PO_4)_2$ formed at mean time. This may take effect in retarding the hydrating of AARS, too. No characteristics of zeolite phases can be identified in this experiment.

In order to understand more about the new phase, samples are also tested using SEM and EDS [6]. The experimental results are revealed in Fig. 4. In observation under SEM, a great number of needle-like hydration products can be seen in AARS paste at early age. The products form a membrane covered on the surface of particles. This may be the intrinsic cause for sodium phosphate to retard the hydration of AARS. The composition of this needle-like phase is analyzed using EDS. The results are shown in Tables 4 and 5.

According to the results of analysis, the formula of the new phase is suggested as following.

$$(Ca, Na)O \cdot (Si, Al)O_2 \cdot y(Ca, Na)SO_4 \cdot xH_2O$$

By comparing Fig. 4(a) with (b), it is also concluded that the content of sodium in products decreases with the

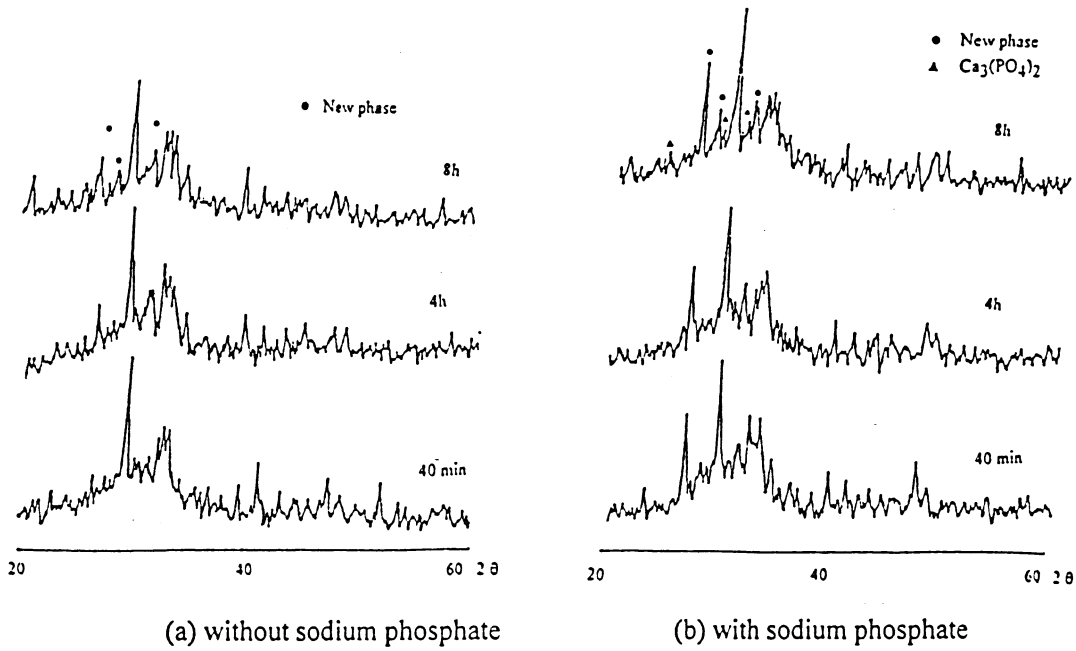

Fig. 3. XRD pattern of AARS.

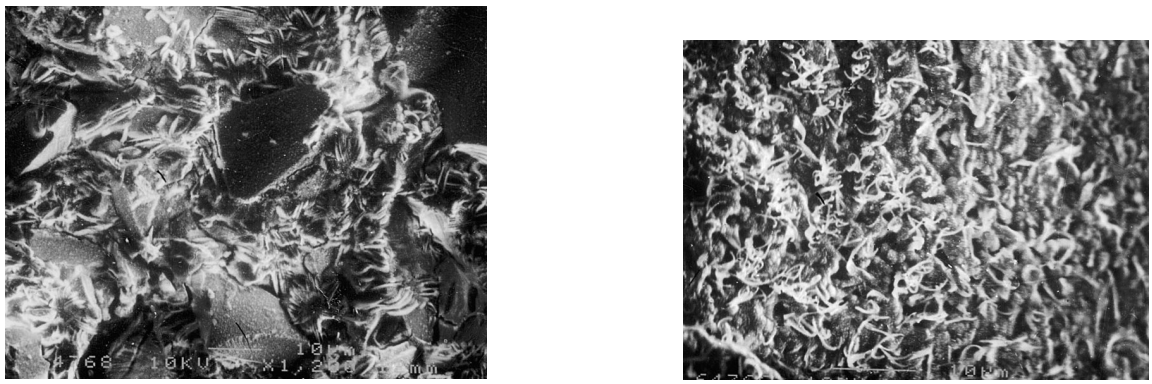

Fig. 4. SEM micromorphology of AARS paste hydrating for 30 min (a) or 1 h (b).

Table 4
Twenty-point average composition analysis results of needle-like products in Fig. 4(a)

Element	Na	Mg	Al	Si	P	S	Ca	Fe
Mass (%)	37.15	0	1.87	17.05	2.41	26.74	12.20	2.58
Mole (%)	45.06	0	2.67	16.99	2.17	23.31	8.51	1.29
Calculated formula	$(Ca,Na)O\cdot(Si,Al)O_2\cdot 2.8(Ca,Na)SO_4\cdot xH_2O$							

Table 5
Twenty-point composition analysis results of needle-like products in Fig. 4(b)

Element	Na	Mg	Al	Si	P	S	Ca	Fe
Mass (%)	15.13	1.22	4.10	37.16	4.36	4.69	30.82	2.53
Mole (%)	19.99	1.54	4.62	40.33	4.27	4.45	23.42	1.38
Calculated formula	$(Ca,Na)O\cdot(Si,Al)O_2\cdot 0.1(Ca,Na)SO_4\cdot xH_2O$							

hydration of AARS. At mean time, there is also P contents in the composition. It may be inferred that there exist some phosphates in the product. These results conform to those of XRD.

4. Conclusion

Sodium phosphate retards the setting and hydration of AARS, and greatly decreases the heat evolution of AARS during hydration. It is an effective retarder of AARS.

It is found through XRD experiment that a new phase forms in AARS paste at early age. The new needle-like product is observed to form a membrane cover on the surface of AARS particles under SEM. It is inferred that sodium phosphate expedites the forming of the new phase attributes to its retarding mechanism.

The formula of the new phase is tested through EDS, and calculated as:

$$(Ca,Na)O\cdot(Si,Al)O_2\cdot y(Ca,Na)SO_4\cdot xH_2O.$$

No zeolite-like hydration products are observed or identified.

References

[1] W.A. Gutteridge, C.D. Pomeroy, Cement in its conventional uses: problems and possibilities, Philos Trans R Soc, London 7 (1983) A310.
[2] D.M. Roy, Advanced cement systems, including CBC, DSP, MDF, Proc 9th Int Congr Chem Cem, New Delhi, India, 1, 1992, pp. 357–380.
[3] B. Talling, J. Brandstetr, Present state and future of alkali-activated slag concretes, Trondheim Conference, Am Concr Inst SP 114 (1989) 1512–1540.
[4] J. Davidovits, What future for Portland cement? Symposium on Cement and Concrete in Global Environment, Chicago, Illinois, USA, (1993) Mar 10–11.
[5] C. Gong, N. Yang, Study on alkali-activated red mud–slag cementitious material, Ind Ital Cem (1998) Nov 898–904.
[6] N. Yang, Testing Methods for Inorganic and Nonmetallic Materials, Press of Wuhan Technology University, Wuhan, 1990.